remote sensing

MDPI

Article

Differentiating among Four Arctic Tundra Plant Communities at Ivotuk, Alaska Using Field Spectroscopy

Sara N. Bratsch [1,*], Howard E. Epstein [1], Marcel Buchhorn [2,3] and Donald A. Walker [2]

Received: 19 September 2015; Accepted: 25 December 2015; Published: 8 January 2016
Academic Editors: Santonu Goswami, Daniel J. Hayes, Guido Grosse, Benjamin Jones, Clement Atzberger and Prasad S. Thenkabail

1 Environmental Sciences Department, University of Virginia, 291 McCormick Road, Charlottesville, VA 22904, USA; hee2b@virginia.edu
2 Alaska Geobotany Center, Institute of Arctic Biology, University of Alaska Fairbanks, 902 N. Koyukuk Dr., Fairbanks, AK 99775, USA; mbuchhorn@alaska.edu (M.B.); dawalker@alaska.edu (D.A.W.)
3 Hyperspectral Imaging Laboratory, Geophysical Institute, University of Alaska Fairbanks, 903 Koyukuk Dr., Fairbanks, AK 99775, USA
* Correspondence: sb9ef@virginia.edu (S.N.B.); Tel.: +1-434-924-4308 (ext. 688) (H.E.E.)

Abstract: Warming in the Arctic has resulted in changes in the distribution and composition of vegetation communities. Many of these changes are occurring at fine spatial scales and at the level of individual species. Broad-band, coarse-scale remote sensing methods are commonly used to assess vegetation changes in the Arctic, and may not be appropriate for detecting these fine-scale changes; however, the use of hyperspectral, high resolution data for assessing vegetation dynamics remains scarce. The aim of this paper is to assess the ability of field spectroscopy to differentiate among four vegetation communities in the Low Arctic of Alaska. Primary data were collected from the North Slope site of Ivotuk, Alaska (68.49°N, 155.74°W) and analyzed using spectrally resampled hyperspectral narrowbands (HNBs). A two-step sparse partial least squares (SPLS) and linear discriminant analysis (LDA) was used for community separation. Results from Ivotuk were then used to predict community membership at five other sites along the Dalton Highway in Arctic Alaska. Overall classification accuracy at Ivotuk ranged from 84%–94% and from 55%–91% for the Dalton Highway test sites. The results of this study suggest that hyperspectral data acquired at the field level, along with the SPLS and LDA methodology, can be used to successfully discriminate among Arctic tundra vegetation communities in Alaska, and present an improvement over broad-band, coarse-scale methods for community classification.

Keywords: Arctic Transitions in the Land-Atmosphere System (ATLAS); North American Arctic Transect (NAAT); hyperspectral; arctic tundra vegetation; vegetation classification

1. Introduction

Remote sensing has allowed for the assessment of changes occurring in arctic vegetation at a variety of spatial and temporal scales [1]. Past studies have mapped vegetation changes at high northern latitudes using aerial photography [2], coarse-scale satellite imagery such as that from the Advanced Very High Resolution Radiometer (AVHRR) [3], and moderate-scale satellite imagery such as that from Landsat platforms [4,5]. The Normalized Difference Vegetation Index (NDVI), a remotely sensed indicator of photosynthetic capacity [6], is one of the most commonly used spectral vegetation indices (SVIs), and is widely available from satellite sensors, such as the AVHRR, the Moderate-Resolution Imaging Spectroradiometer (MODIS), and the various Landsat sensors that capture spectral information in a few

broad spectral bands. NDVI provides an accessible means to monitor changes in the quantity of green vegetation on broad spatial and relatively long temporal scales. NDVI is therefore frequently used to evaluate vegetation changes in high latitude environments [1,6–16]. One of the previous analyses at the site of interest for this study (Ivotuk, Alaska) showed that, at the landscape scale, broad-band NDVI obtained by averaging hyperspectral bands across red and near infrared (NIR) regions had the greatest peak growing season values for shrub tundra (ST), compared to three other tundra plant communities [17]. While NDVI may be useful for separating some communities at peak growing season, it may be problematic during the early or late growing season when vegetation communities are more similar (Figure 1). Broad-band NDVI is calculated from two coarse regions of the spectrum [6], which can potentially obscure important information in spectra that might be useful for differentiating among vegetation communities.

Vegetation changes in the Arctic are likely occurring at fine spatial and spectral scales and at the level of individual species, the monitoring of which may benefit from the use of hyperspectral remote sensing [18]. More defined regions of the visible and near infrared spectra than those captured by multispectral sensors, including those outside the range of NDVI bands, can be used to identify functional and structural properties of vegetation communities [19,20]. Tundra vegetation communities are often comprised of bare soils or large quantities of non-vascular components (mosses and lichens) that affect the spectral signatures of vegetation communities [10,21]. Ground-based remote sensing data have been collected from a variety of sites throughout the North Slope of Alaska [9,18,22–24]; this hyperspectral remote sensing (also known as imaging spectroscopy) information has been useful in differentiating among distinct vegetation communities in the Arctic [18], as well as between vascular and non-vascular vegetation [24]. A discriminant analysis of peak season data from Barrow, Alaska, found moss and vascular plant spectra to have similar reflectances in the green and NIR wavelengths, while lichens had higher reflectance in the visible wavelengths and greater variability among species-specific reflectances [24]. Dead biomass in the Arctic also influences NDVI and reflectivity spectra. This factor becomes more influential as shrubs begin to dominate these systems, and their leaf litter covers more low-lying plants [25,26].

The objective of this paper is to differentiate among Alaskan Arctic tundra plant communities through the use of field spectroscopy and to identify diagnostic wavelength regions for discriminating among these communities at different phenological stages. We first develop a model for identifying different vegetation communities at Ivotuk, Alaska using hyperspectral data; this discrimination model is then applied to five other sites on the North Slope of Alaska to test its utility in identifying tundra vegetation across geographical space.

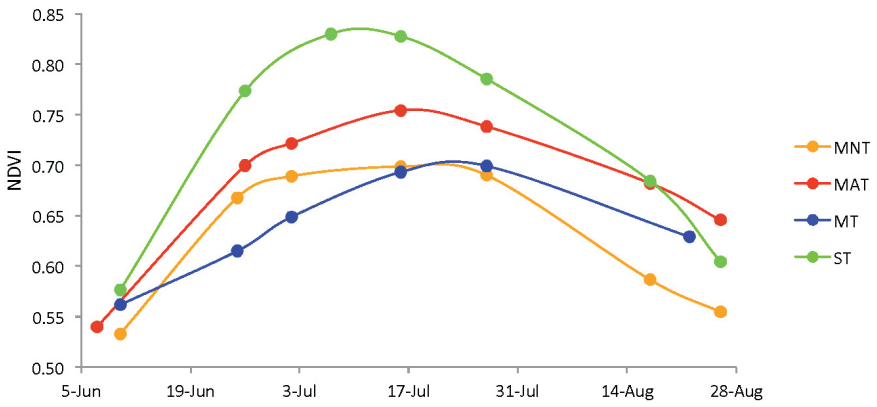

Figure 1. NDVI throughout the 1999 growing season for four different vegetation communities at Ivotuk, Alaska. Adapted from [17]. Measurements were taken using an Analytical Spectral Devices FieldSpec spectro-radiometer.

2. Materials and Methods

2.1. Arctic Change

The Arctic has warmed at a greater rate than the rest of the globe through a process known as polar amplification [22,27,28]. This warming phenomenon is largely attributed to a reduction in sea-ice extent and concomitant changes in albedo [29,30]. From 1981–2012, the change in global temperature was observed to be ~0.17 °C per decade [31], while warming in the Arctic (>66°N) was approximately 0.60 ± 0.07 °C per decade [30]. Satellite observations from 1982–2008 have shown greater warming trends in the North American Arctic (+30%) than in the Eurasian Arctic (+16%) based on the Summer Warmth Index (SWI), which is defined as the sum of average monthly surface temperatures above freezing [32]. Temperature changes have likely caused a lengthening of the growing season in the Arctic [14,33], and associated vegetation changes such as greater vegetation biomass [7,32,34,35], changes in vegetation composition and leaf area index (LAI) [36], and an increase in shrub cover [15,37–39]. Vegetation greenness as determined by the NDVI has increased approximately 9% in the North American Arctic, while greenness in the Eurasian Arctic has increased by only 2% since 1982 [32]. This recent increase in NDVI in the Arctic has been linked to greater plant biomass [7,40], increased photosynthetic capacity, and an expansion of shrubs [41,42]. Substantial increases in biomass are predominately seen in subzones C–E [43,44], the three southernmost tundra subzones as identified in the Circumpolar Arctic Vegetation Map (CAVM) [43,44], with an average increase in biomass of 19.8% from 1982–2010 [7]. The total increase in Alaskan tundra biomass during this time period was 7.8% [7]. Enhanced spectral resolution in remote sensing data could potentially help identify the nuances of these dynamics in plant biomass.

2.2. Vegetation Types throughout the North Slope of Alaska

The North Slope of Alaska extends from the Brooks Mountain Range to the Arctic Ocean [45] and is largely dominated by either moist acidic tundra (MAT) or moist nonacidic tundra (MNT) [5]. Soil acidity differentiates MAT from MNT communities, with MAT occurring on soils with pH < 5.0–5.5, and MNT occurring on soils with pH $\geqslant$ 5.0–5.5 [16,46]. MAT often occurs in areas with rolling topography and gravelly or silty soils overlain by an organic mat of up to 20 cm [47]. MAT is dominated by dwarf erect shrubs such as *Betula nana*, graminoid species such as *Eriophorum vaginatum*, and acidophilous mosses (e.g., *Aulacomium turgidum*) [5,46]. MNT communities tend to occur along rivers and in the more northern Arctic Foothills and Coastal Plains [42]. Mosses, graminoids (e.g., *Carex bigelowii*), and prostrate dwarf shrubs (e.g., *Dryas integrifolia*) dominate these communities [34] on calcium-rich, nonacidic (neutral pH) soils [48,49]. *Betula nana* is absent from MNT communities due to its affinity for acidic soils [5]. MNT differs in ecosystem structure and function from MAT, and generally has lower NDVI, LAI, and rates of photosynthesis and ecosystem respiration compared to MAT communities [49–51].

Other vegetation types on the North Slope of Alaska include shrub tundra (ST) and mossy tussock tundra (MT). Shrub tundra is dominated by erect shrubs such as *Salix alaxensis* and *Betula nana*, and is interspersed with graminoids, forbs, lichens, and mosses. Low shrub areas include shrubs approximately 40–60 cm in height, whereas heath shrub landscapes include shrubs approximately 10–20 cm in height [52]. On average, ST communities have lower albedo, lower summer soil temperatures, shallower summer active layer depths, and greater summer CO_2 exchange and sensible heat flux than other vegetation types [2]. Mossy tussock tundra is typified as an MAT community of tussock-forming sedges (e.g., *E. vaginatum*) with abundant *Sphagnum* mosses, and contributes greatly to biomass quantities in the Alaskan Arctic [53].

2.3. Study Sites

The primary study site of Ivotuk, Alaska (68.49°N, 155.74°W) is located on the North Slope of the Brooks Mountain Range [8,17,54] and was one of seven sites established as part of the Arctic

Transitions in the Land-Atmosphere System (ATLAS) project [16,55,56]. Ivotuk is part of the Western Alaska Transect that starts in the north at Barrow and goes south through Atqasuk and Oumalik to Ivotuk [16,42,55,57]. The Eastern Alaska Transect starts in the north at Prudhoe Bay and ends at Toolik Lake, a Long-Term Ecological Research (LTER) site [46,58,59]. Ivotuk is located in bioclimatic subzone E, the warmest and southernmost of the five tundra subzones (Figure 2) [56]. Ivotuk is largely a tussock tundra ecosystem also dominated by deciduous shrubs [16] (Figure 3). It is located at an elevation of approximately 550 m [54], and is considered comparable to the Toolik Lake site [8]. The site received an average annual rainfall of 202 mm, had a July maximum temperature of approximately 12 °C and an annual temperature of −10.9 °C with a 110-day growing season from 1991–2001, a time period including the sampling period for the Ivotuk vegetation data [8,17,42]. Aerial vegetation coverage is nearly 100% for Ivotuk, and all four plant communities in this study—MAT, MNT, MT, and ST—occur within a 2 km^2 area [17]. ST had the greatest total aboveground peak growing season biomass (1291 g/m^2). MAT had a total aboveground biomass of 842 g/m^2 during peak growing season, while MT had a total of 804 g/m^2, and MNT had a total of 725 g/m^2 [17]. Moss was the dominant contributor to biomass in MNT communities. Deciduous shrubs were the most dominant biomass component in ST communities, and graminoids were the most dominant contributor in MAT and MT communities (Table 1).

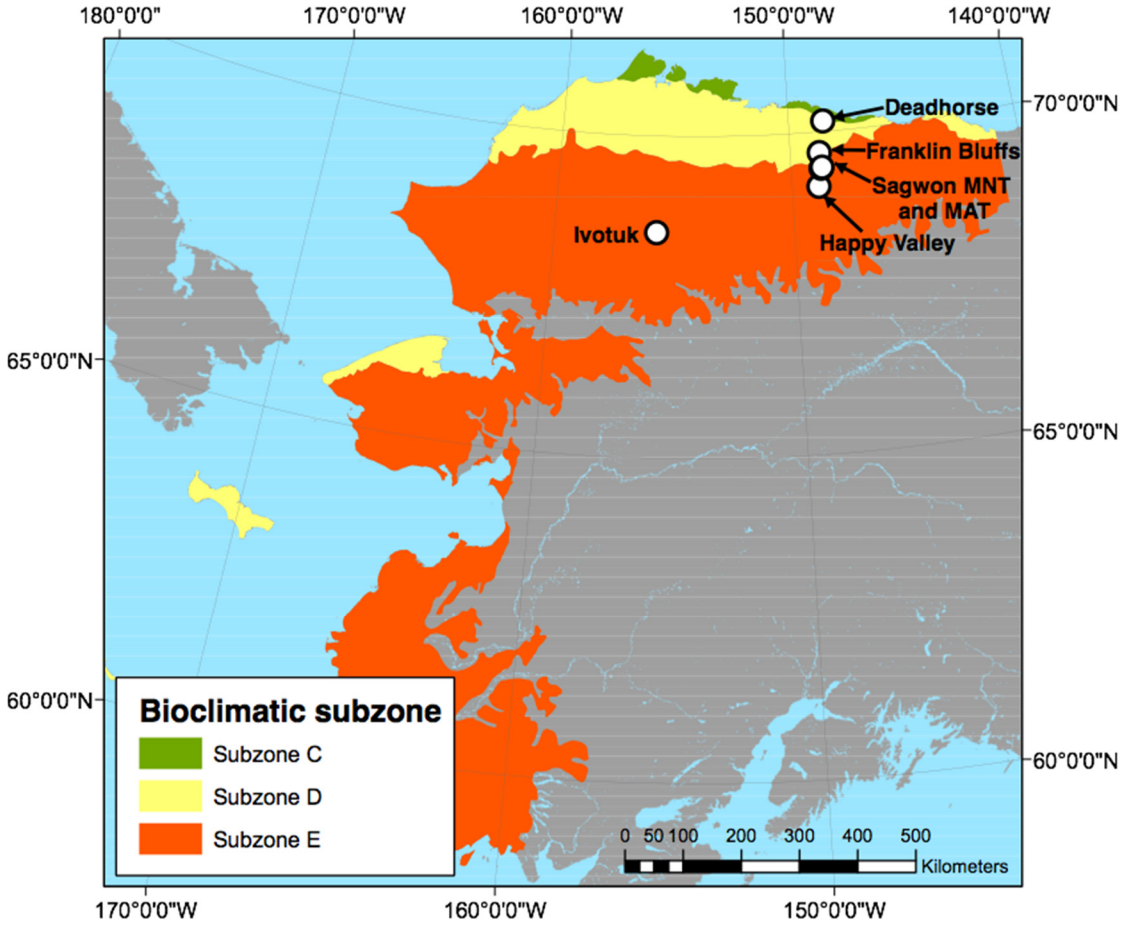

Figure 2. Location of Ivotuk, Deadhorse, Franklin Bluffs, Sagwon-MNT, Sagwon-MAT, and Happy Valley sites on the North Slope of Alaska within the Alaskan bioclimatic subzones of the Circumpolar Arctic Vegetation Map [44].

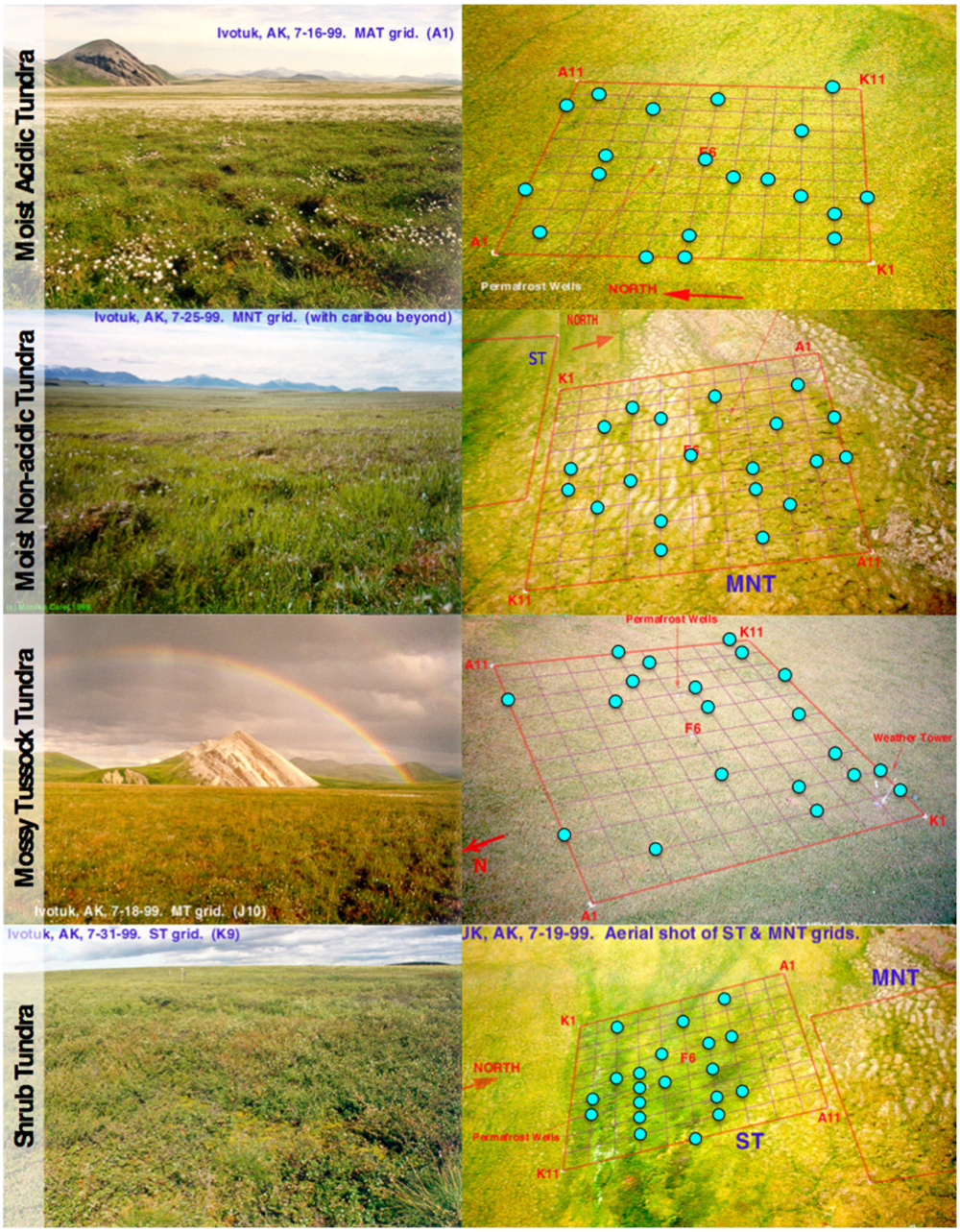

Figure 3. The four vegetation communities at Ivotuk, Alaska along with the grid and spectral sampling locations. Each point represents one sampling gridpoint. Study site images were taken between 16–31 July 1999. All grid images were taken on 19 July 1999 [60].

Table 1. Biomass percentages by plant functional type (PFT) during early (7 June–7 July) and peak (16 July–17 August) growing season at Ivotuk, Alaska.

PFT	Early				Peak			
	MAT (%)	MNT (%)	MT (%)	ST (%)	MAT (%)	MNT (%)	MT (%)	ST (%)
Deciduous shrub	15.6	3.7	3.6	64.1	18.8	5.1	3.6	55.9
Evergreen shrub	22.1	9.4	14.5	0.2	23.7	14.4	14.7	1.6
Forb	0.2	4.2	0.0	0.7	0.4	3.3	0.0	1.1
Graminoid	32.0	9.4	35.9	3.8	27.5	12.2	36.1	10.4
Lichen	4.9	3.0	3.1	1.3	5.7	3.6	3.3	2.4
Moss	25.2	70.3	42.4	29.9	23.9	61.5	42.4	28.6

To evaluate the differentiation model developed with the data from Ivotuk, we used a series of additional sites along the Dalton Highway on the North Slope of Alaska from which hyperspectral data have also been collected [18]. The sites of Happy Valley (69.15°N, 148.85°W), Sagwon-MAT (69.43°N, 148.70°W), Sagwon-MNT (69.43°N, 148.7°W), Franklin Bluffs (69.67°N, 148.72°W), and Deadhorse (70.16°N, 148.46°W) are located along the Dalton Highway in Alaska and are part of the North American Arctic Transect (NAAT). Detailed descriptions of the sites can be found in [22,61–64]. Deadhorse, Franklin Bluffs, and Sagwon-MNT are MNT communities; Happy Valley and Sagwon-MAT are both MAT communities. Deadhorse is the northernmost site, occurs in the transition between subzones C and D, and was atypically wet during the 2012 data collection period [18]. Franklin Bluffs is in subzone D, and Sagwon MAT and MNT occur at the transition zone between subzones D and E. Happy Valley is the southernmost site, is located in subzone E, and most closely resembles the primary study site of Ivotuk.

2.4. Data Collection

One 100 m^2 vegetation grid was established in each community at Ivotuk for a total of four grids. Field spectroscopy data were collected during the 1999 growing season at biweekly intervals from 5 June–17 August. Spectroscopy data were grouped into early or peak growing season as determined by seasonal NDVI curves (Figure 1, Table 2). Data were grouped to avoid issues with low sample size for each of the individual sampling dates. Spectral measurements were taken using an Analytical Spectral Devices FieldSpec spectro-radiometer with a spectral resolution of 1.42 nm and a spectral range from 330–1062 nm. The sensor was held at nadir approximately 1.5 m above the vegetation surface, producing a 0.35 m^2 footprint with a 25° field of view [17]. Spectral measurements were collected from ten random gridpoints established in each of the four vegetation grids. Spectra were taken from an additional ten gridpoints during peak growing season. Both the MNT and the ST grids exhibited some within-grid heterogeneity that was likely to influence the results. Within these grids, we stratified the random sampling in such a way that we were sampling only vegetation that was representative of that particular community. Four replicate spectral measurements were taken at each gridpoint by moving 1 m in each cardinal direction from the actual gridpoint. Replicates were averaged to create the ten gridpoint spectral measurements per vegetation community per biweekly interval.

Data from the study sites of Deadhorse, Franklin Bluffs, Sagwon-MNT, Sagwon-MAT, and Happy Valley were collected during the 2012 growing season from 29 June to 11 July within the EyeSight-NAAT-Alaska expedition [18,65]. Measurements were taken using two Spectra Vista Corporation GER1500 portable field spectro-radiometers with a spectral resolution of 1.5 nm and a spectral range from 330–1050 nm [18]. One 100 m^2 vegetation grid was sampled from each of the study sites. The grid was divided into 1 × 1 m quadrats for a total of 100 observations. These values were then averaged to produce mean reflectances per site.

Table 2. Sampling dates and total number of observations per vegetation community during the early (7 June–7 July) and peak (16 July–17 August) 1999 growing season at Ivotuk, Alaska.

Growing Season	MAT	MNT	MT	ST
Early	7 June, 26 June, 2 July (n = 42)	10 June, 25 June, 2 July (n = 45)	10 June, 25 June, 2 July (n = 41)	10 June, 26 June, 7 July (n = 37)
Peak	16 July, 27 July, 17 August (n = 40)	16 July, 27 July, 17 August (n = 43)	16 July, 27 July (n = 33)	16 July, 27 July, 7 August (n = 33)

2.5. Spectral Processing

All spectra were evaluated visibly for potentially bad data. Outliers were removed from the dataset in an effort to achieve a more diagnostic spectral signature; this resulted in an underrepresentation of MT and ST during peak growing season. Spectroscopy data were resampled to 5 nm wide hyperspectral

narrowbands ranging from 400–1000 nm. Resampling increases the signal-to-noise ratio, reduces redundancy issues among predictor variables, and makes the results potentially more transferable from Ivotuk to the five other Alaskan sites, for which data were collected with a different spectro-radiometer.

In addition to the original reflectances, data were also analyzed using continuum removal. Continuum removal normalizes spectra by establishing a baseline from which to compare absorption features [66], and this methodology can be used to effectively discriminate among vegetation types [18]. Continuum removal for three absorption feature regions (blue, red, and water) was performed using ENVI (Exelis Visual Information Solutions, Boulder, CO, USA). Averaged reflectances per vegetation community were used for continuum-removal analysis of the three absorption features: (1) blue absorption (400–550 nm); (2) red absorption (560–750 nm); and (3) water absorption (930–1055 nm). Spectral metrics such as maximum band depth, HNB at maximum band depth, width of the absorption feature at half maximum absorption depth, and area of the absorption feature were analyzed for these three features [67].

2.6. Data Analysis

To decrease the amount of redundant hyperspectral narrow bands (HNBs), overcome the Hughes's phenomenon [68,69], and identify optimal HNBs for distinguishing among arctic vegetation communities, we used a two-step sparse partial least squares (SPLS) and linear discriminant analysis (LDA). SPLS regression was done using the SIMPLS algorithm from the "spls" package in R [70]. SPLS is a variable selection and dimension reduction technique that is useful for spectroscopic analysis, as it is unaffected by issues such as high collinearity among predictor variables and cases where $p > n$. The resulting latent vectors are in terms of the original HNBs as a result of the sparsity parameter in SPLS [71].

The HNBs with the greatest loading coefficients from the SPLS (top 10%) were then put through an LDA to discriminate among the four vegetation communities at Ivotuk. A simple random sample of approximately one-half of the Ivotuk data were used as a training set for the model, and then the model was applied to the remaining test set of Ivotuk data. Following this, peak growing season data from Ivotuk were used as the training set and tested against the five study sites of Deadhorse, Franklin Bluffs, Sagwon-MNT, Sagwon-MAT, and Happy Valley.

3. Results

3.1. Sparse Partial Least Squares (SPLS) and Linear Discriminant Analysis (LDA)

SPLS identified eight optimal HNBs during early growing season and twelve optimal HNBs during peak growing season (Table 3). The majority of HNBs for early and peak growing season were in the NIR wavelength region (Figure 4), and the spectral locations of the most significant HNBs differ seasonally. HNBs in the blue, green, and NIR load highest during the early growing season, whereas HNBs in the NIR load highest during the peak growing season. Overall classification accuracy of the LDA was greater during peak growing season at 94% compared to early growing season at 84% (Table 4; Figure 5). MT was the best classified community during early growing season at 100%. ST had the lowest classification accuracy during early growing season at 65%. MNT, MT, and ST were all classified at 100% during peak growing season. MAT was classified at 80% during peak growing season.

Table 3. Top ten percent of significant hyperspectral narrowbands (HNBs) for all four vegetation communities and overall classification accuracy of the linear discriminant analysis (LDA) using the optimal HNBs. All Wilks's lambda values are significant ($p < 0.001$).

Sampling Period	Significant HNBs (nm)	Wilks' Lambda	Sum of Eigenvalues	Overall Classification Accuracy Using the Optimal HNBs Only (%)
Early	405, 505, 690, 770, 840, 905, 920, 980	0.03	8.41	84
Peak	405, 450, 790, 795, 800, 845, 850, 910, 940, 975, 980, 990	0.01	12.39	94

Table 4. Confusion matrices and classification accuracies at Ivotuk, Alaska using the top ten percent of significant hyperspectral narrowbands (HNBs).

Classification Accuracy (%)	Early Growing Season					Classification Accuracy (%)	Peak Growing Season				
		MAT	MNT	MT	ST			MAT	MNT	MT	ST
73	MAT	16	-	4	2	80	MAT	16	-	-	4
92	MNT	1	2	1	-	100	MNT	-	23	-	-
100	MT	-	-	21	-	100	MT	-	-	13	-
65	ST	2	-	4	11	100	ST	-	-	-	13

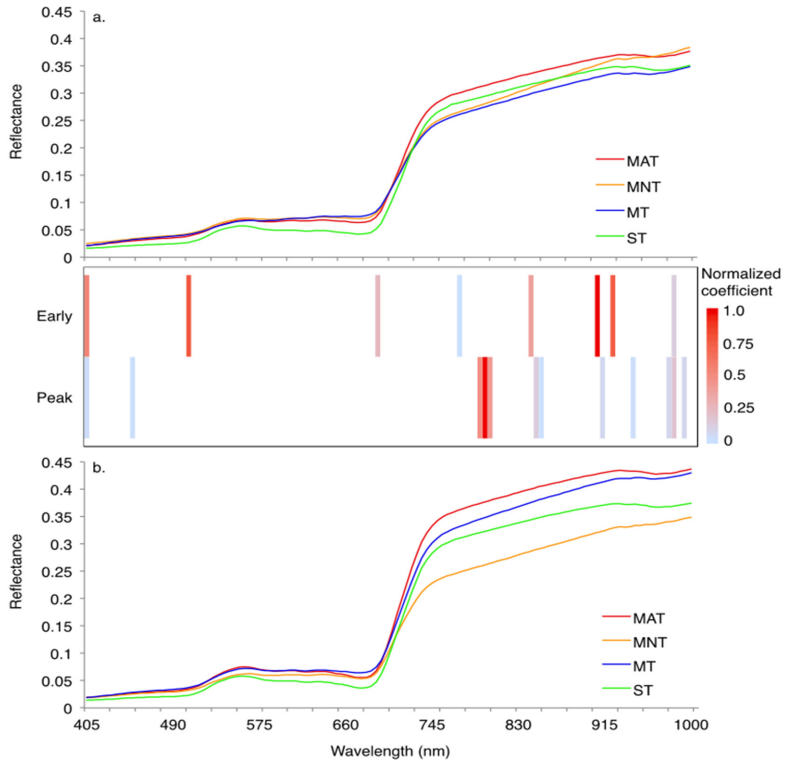

Figure 4. Mean reflectance spectra for the four vegetation communities during early (**a**) and peak (**b**) growing season at Ivotuk, Alaska in 1999. Reflectance spectra are shown along with the top ten percent of optimal hyperspectral narrowbands (HNBs) and their normalized coefficients for the first discriminant function.

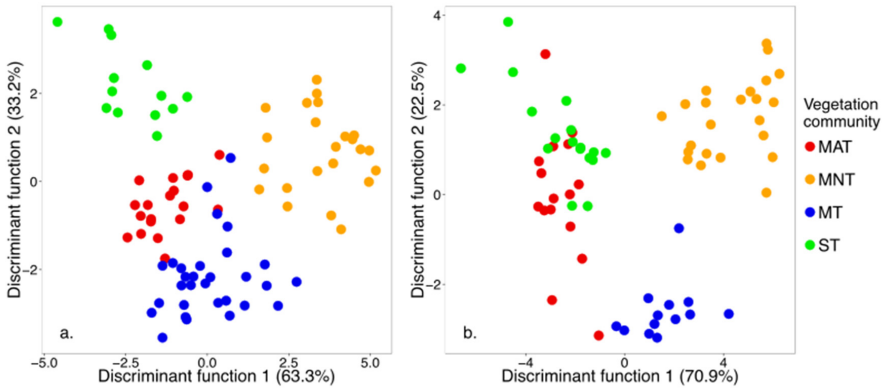

Figure 5. First two functions derived from linear discriminant analysis for the four vegetation communities at Ivotuk, Alaska using the top ten percent of optimal hyperspectral narrowbands (HNBs) during early (**a**) and peak (**b**) growing season.

3.2. Continuum Removal

Continuum-removed reflectance spectra were examined in the blue, red, and water absorption features. Continuum-removed reflectance spectra did not always exhibit clear distinctions among the four vegetation communities during early (Figure 6) or peak growing season (Figure 7). Maximum absorption depth for the blue absorption feature was found at 495–500 nm for all vegetation communities during early and peak growing season (Table 5). Maximum absorption depth occurred at 680 nm for the red absorption feature, and 965–980 nm for the water absorption feature. ST had the greatest values for the three spectral metrics of maximum band depth, full width at half maximum band depth, and area of absorption feature. Scaled continuum-removed reflectances indicate that differences among vegetation community types are most pronounced in the 400–500 nm region of the blue absorption feature. Differences are most pronounced in the 560–680 nm range in the red absorption feature, and between 930–945 nm for the water absorption feature.

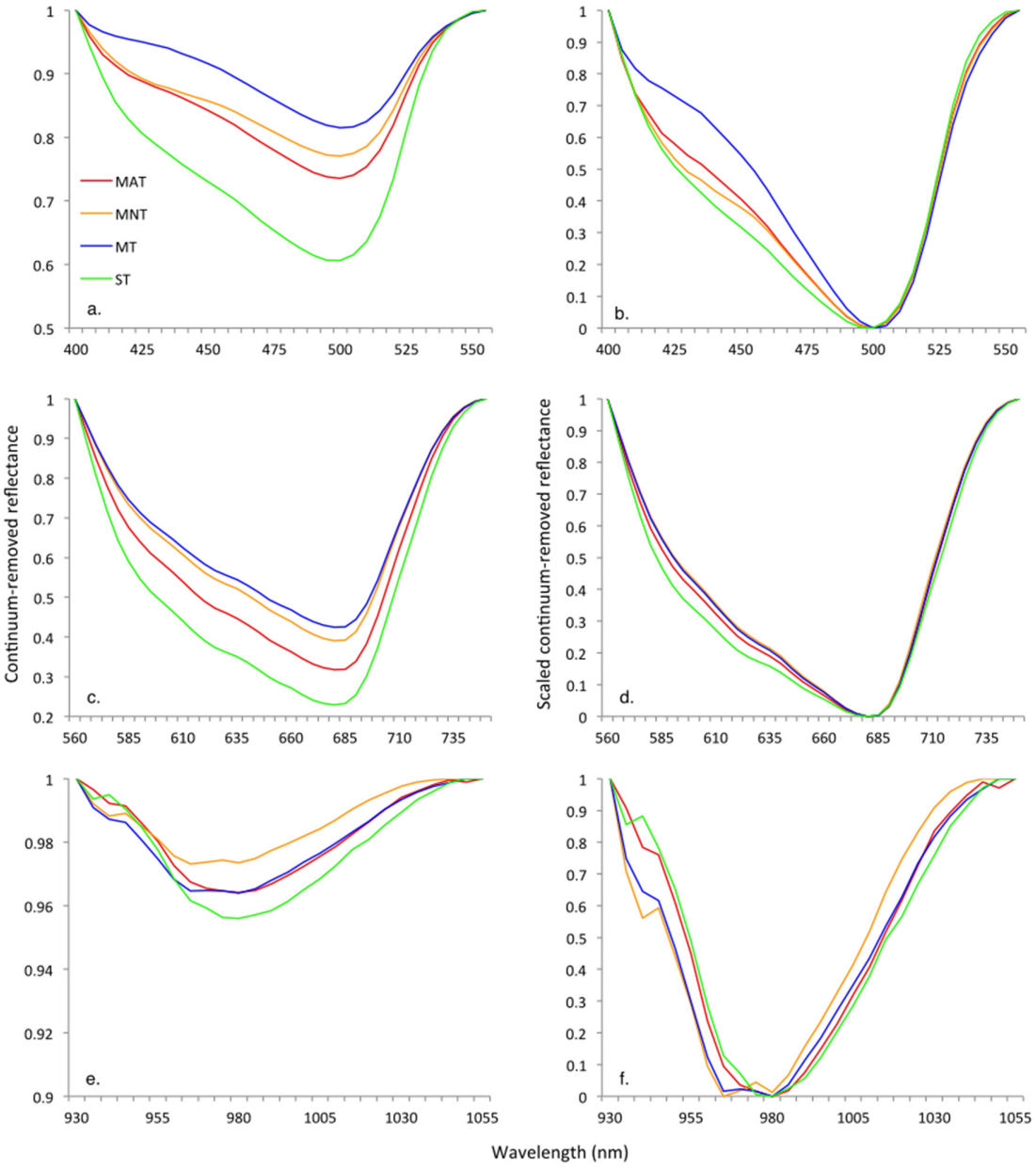

Figure 6. Average continuum-removed and scaled continuum-removed reflectance spectra at Ivotuk, Alaska for the blue (**a**,**b**), red (**c**,**d**), and water (**e**,**f**) absorption features during early growing season.

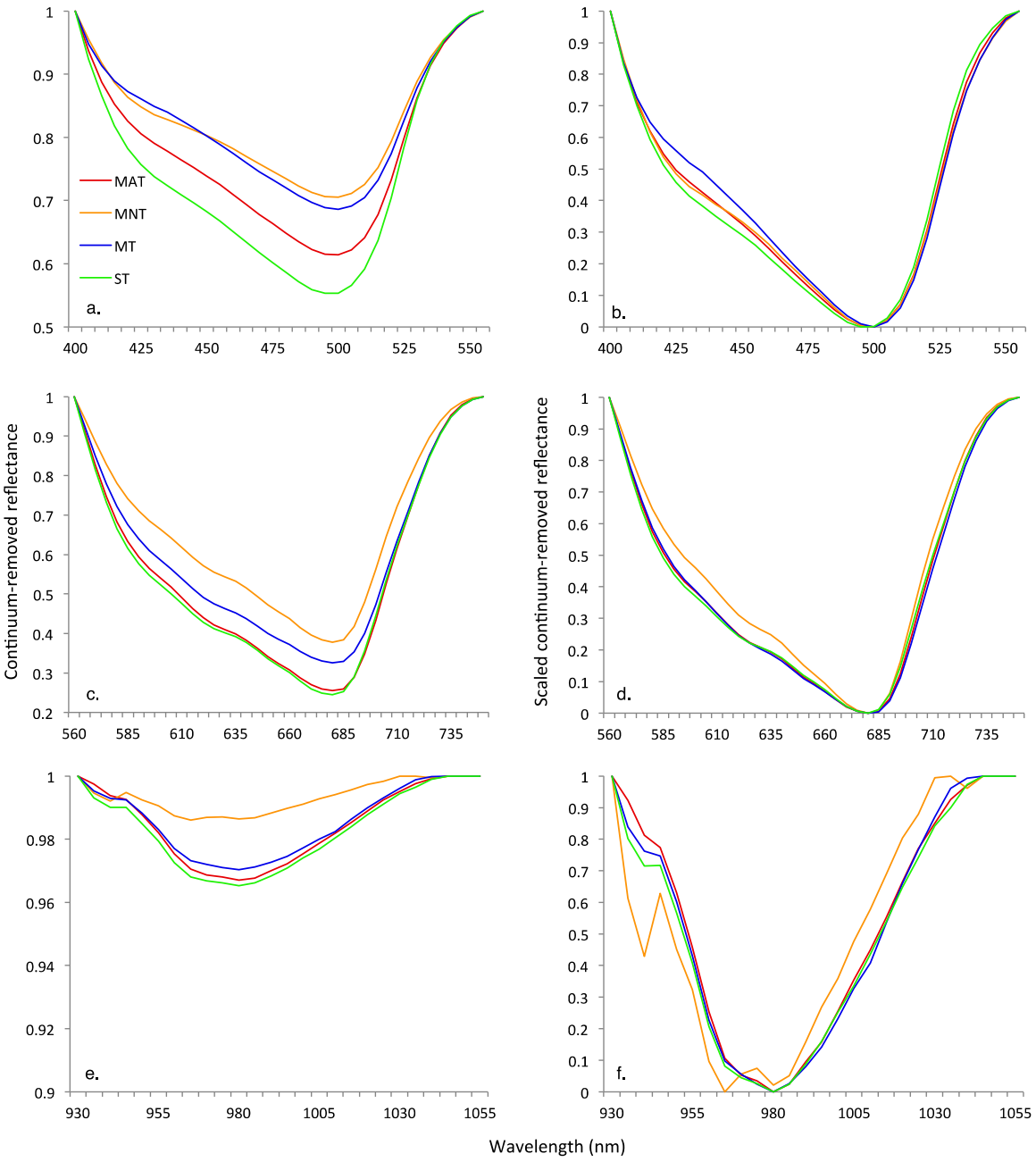

Figure 7. Average continuum-removed and scaled continuum-removed reflectance spectra at Ivotuk, Alaska for the blue (**a**,**b**), red (**c**,**d**), and water (**e**,**f**) absorption features during peak growing season.

Table 5. Spectral metrics from continuum-removal analysis for the blue, red, and water absorption features at Ivotuk.

		Blue				Red				Water			
Growing Season	**Vegetation Community**	**HNB of Maximum Depth (nm)**	**Maximum Band Depth**	**Full Width at Half Maximum Band Depth (nm)**	**Area of Absorption Feature**	**HNB of Maximum Depth (nm)**	**Maximum Band Depth**	**Full Width at Half Maximum Band Depth (nm)**	**Area of Absorption Feature**	**HNB of Maximum Depth (nm)**	**Maximum Band Depth**	**Full Width at Half Maximum Band Depth**	**Area of Absorption Feature**
Early	MAT	500	0.26	87.53	22.8	680	0.68	125.01	78.1	980	0.04	61.66	2.2
	MNT	500	0.23	96.52	20.2	680	0.61	120.23	67.6	965	0.03	65.44	1.7
	MT	500	0.18	71.53	14.4	680	0.58	121.64	64.6	980	0.04	67.04	2.4
	ST	500	0.39	98.56	35.6	680	0.77	131.28	92.2	980	0.04	60.69	2.8
Peak	MAT	500	0.39	101.14	35.5	680	0.74	125.02	84.6	980	0.03	58.99	2.0
	MNT	500	0.29	102.65	27.2	680	0.62	113.72	65.7	965	0.01	59.64	0.8
	MT	500	0.31	92.98	28.2	680	0.67	125.20	77.2	980	0.03	62.96	1.8
	ST	495	0.45	103.67	41.6	680	0.76	125.79	86.0	980	0.03	40.70	2.2

3.3. Predicting Vegetation Community Types at the Five Dalton Highway Test Sites

Peak growing season spectra from Ivotuk were used as a training set to create models that were then used to predict plant community types at the five other Alaska sites. Only MAT and MNT vegetation communities were used for this analysis as MT and ST communities were not sampled at the other sites. This subset of the Ivotuk data was put through the two-step SPLS and LDA to determine optimal HNBs. The resulting model was then applied to the five sites of Deadhorse, Franklin Bluffs, Sagwon-MNT, Sagwon-MAT, and Happy Valley.

This analysis identified nine optimal HNBs. Bands in the red edge were the most common and the most significant to the model (Table 6, Figure 8). Classification accuracy was better for MAT communities than MNT communities, and generally better at sites more similar to, and geographically nearer to, Ivotuk. Sagwon-MAT was the best classified community (91%), followed by Happy Valley (90%). The closest MNT community to Ivotuk is Sagwon MNT, which had the greatest classification accuracy of the three MNT communities (70%). Both Deadhorse and Franklin Bluffs are more northern than the rest of the sites, and had similar classification accuracies of 56% and 55%, respectively.

Table 6. Optimal hyperspectral narrowbands (HNBs) for the five Dalton Highway sites and overall classification accuracy of the linear discriminant analysis (LDA) using the top ten percent of optimal HNBs.

Optimal HNBs (nm)	Site and Community Classification	Overall Classification Accuracy Using the Optimal HNBs Only (%)
470, 685, 690, 695, 710, 715, 760, 935, 980	Deadhorse	56
	Franklin Bluffs	55
	Sagwon-MNT	70
	Sagwon-MAT	91
	Happy Valley	90

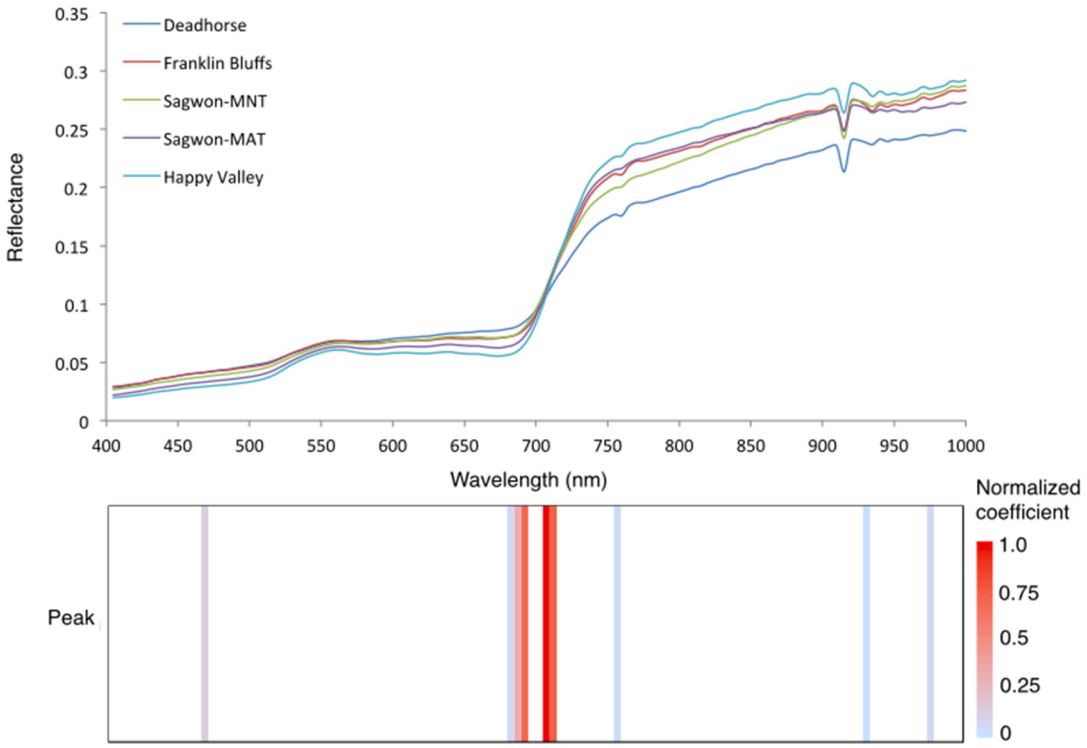

Figure 8. Mean reflectance spectra for the five Dalton Highway test sites. Reflectance spectra are shown along with the top ten percent of optimal hyperspectral narrowbands (HNBs) and their normalized coefficients for the first discriminant function.

4. Discussion

This study uses HNBs and a two-step SPLS and LDA approach to differentiate among vegetation communities at Ivotuk, Alaska. This differentiation model was then applied to the sites of Deadhorse, Franklin Bluffs, Sagwon-MNT, Sagwon-MAT, and Happy Valley. Continuum-removal findings from Ivotuk are similar to other vegetation studies along the North Slope of Alaska that have identified maxima in the blue and red absorption features. Past research on MAT and MNT vegetation communities has identified absorption maxima of 500 nm and 680 nm for the Dalton Highway data used in this study [18]. Findings at Ivotuk are similar to these, with a chlorophyll and carotenoid absorption maximum occurring between 495 and 500 nm, and a second chlorophyll maximum at 680 nm (Figures 6 and 7). The greatest changes in maximum band depth from early to peak growing season were found in the blue absorption feature, indicating greater absorption by chlorophyll and carotenoids during peak growing season.

HNBs located in areas associated with pigments (400–700 nm) had greater linear discriminant coefficients and were more frequently found to be significant during the early growing season. HNBs associated with structural tissue (NIR) were more significant during peak growing season, indicating an increased reliance on vegetation structure and morphological differences among species to differentiate tundra communities during peak growing season. Separability at Ivotuk relied heavily on HNBs outside the typical range of broad-band NDVI. Although HNBs in the NIR were significant, they were never used in a model that also included the red wavelengths. Furthermore, the most significant bands for the Dalton Highway test sites were located in the red edge (680–725 nm), which is typically outside the range of broad-band NDVI. Whereas the vegetation community reflectance at Ivotuk would appear homogeneous with regard to NDVI outside of the peak growing season [17], this study shows that hyperspectral remote sensing data can be used to discriminate among these vegetation communities during the early growing season. The communities of MAT and ST at Ivotuk were the most compositionally similar with regard to the ratio of vascular to non-vascular vegetation, and were the most commonly misclassified during early and peak growing season at Ivotuk. MAT and ST are comprised of approximately 70% vascular plant and 30% non-vascular. MNT has the inverse composition, and MT composition is almost equal between vascular and non-vascular vegetation, and was the only vegetation community never misclassified at Ivotuk. During peak growing season, MAT was exclusively misclassified as ST, highlighting the importance of vegetation structure for tundra community discrimination during peak growing season.

Among the four vegetation types at Ivotuk, ST had the lowest reflectances in the visible spectrum during both early and peak growing season, and MAT had the greatest absolute reflectances for both early and peak growing season. Differences among vegetation communities in the NIR wavelength region occurred during the early growing season, yet were amplified during peak growing season. Other research in the Alaskan Arctic has identified five bands useful for discriminating among vascular and non-vascular vegetation located in the blue, red, and NIR regions [24]. Our study suggests that similar regions of the spectrum can be used to discriminate among vegetation communities also using hyperspectral remote sensing data.

The MAT vegetation types at Ivotuk are most similar to the southernmost test site of Happy Valley. Reflectances in the NIR were greater at Ivotuk than Happy Valley and the other four Dalton Highway test sites. Happy Valley had the lowest reflectances in the visible regions and the highest reflectances in the NIR wavelength regions of the Dalton Highway sites. Sagwon-MNT is the most similar MNT site to the MNT grid at Ivotuk, and like the MNT spectral signature at Ivotuk, had lower reflectances in the NIR than other sites with the exception of Deadhorse, which was unusually wet during the data collection period. Sagwon-MNT had lower reflectances in the NIR than the MNT community at Ivotuk, and greater reflectance in the red trough. Franklin Bluffs and Sagwon MAT exhibited similar reflectances in the NIR, but differed in the visible wavelength region, where reflectance for Sagwon MAT more closely mirrored Happy Valley, the only other Dalton Highway MAT community.

5. Conclusions

This study presents an example of the potential for hyperspectral remote sensing to improve upon the classification of tundra vegetation communities in the Arctic. Field research in the Arctic is difficult and expensive. Ground-based remote sensing studies are critical, as they allow for the development of spectral relationships that can then potentially be extrapolated to satellite remote sensing. The discriminability of MAT, MNT, MT, and ST communities is improved upon through the use of hyperspectral remote sensing in this study. Hyperspectral remote sensing allows for the inclusion of both a wider range of spectral data and finer resolution spectral data than traditional multi-spectral approaches. Establishing these relationships allows for the identification of HNBs on hyperspectral satellites that may be valuable for distinguishing among vegetation communities. Such forthcoming projects include the NASA Hyperspectral Infrared Imager (HyspIRI) and the German Environmental Mapping and Analysis Program (EnMAP). Establishing the spectral differences among these vegetation communities using field spectroscopy data facilitates the potential for monitoring of changes occurring in vegetation communities as a result of increasing temperatures in the Arctic.

Acknowledgments: Fieldwork at Ivotuk was conducted as part of the Arctic Transitions in the Land-Atmosphere System (ATLAS) project (NSF OPP-9908829). This data analysis was funded as part of the NASA Pre-ABoVE (Arctic Boreal Vulnerability Experiment) project (Grant NNX13AM20G) and the National Fish and Wildlife Foundation. Fieldwork for the Dalton Highway sites was conducted as part of the hy-ARC-VEG (hyperspectral method development for ARCtic VEGetation biomes). Heather A. Landes contributed to the production of tables and figures for this manuscript.

Author Contributions: Walker and Epstein conceived, designed, and performed the experiments. Bratsch and Buchhorn designed the data analysis and analyzed the data. Bratsch and Epstein wrote the paper with assistance from Buchhorn and Walker.

Conflicts of Interest: The authors declare no conflict of interest.

References

1. Stow, D.A.; Hope, A.; McGuire, D.; Verbyla, D.; Gamon, J.; Huemmrich, F.; Houston, S.; Racine, C.; Sturm, M.; Tape, K.; *et al*. Remote sensing of vegetation and land-cover change in arctic tundra ecosystems. *Remote Sens. Environ.* **2004**, *89*, 281–308. [CrossRef]
2. Sturm, M.; Schimel, J.P.; Michaelson, G.J.; Welker, J.M.; Oberbauer, S.F.; Liston, G.E.; Fahnestock, J.; Romanovsky, V.E. Winter biological processes could help convert arctic tundra to shrubland. *BioScience* **2005**, *55*, 17–26. [CrossRef]
3. Walker, D.A. An integrated vegetation mapping approach for northern Alaska (1:4 m scale). *Int. J. Remote Sens.* **1999**, *20*, 2895–2920. [CrossRef]
4. Silapaswan, C.; Verbyla, D.; McGuire, A.D. Land cover change on the Seward Peninsula: The use of remote sensing to evaluate the potential influences of climate warming on historical vegetation dynamics. *Can. J. Remote Sens.* **2001**, *27*, 542–554. [CrossRef]
5. Muller, S.V.; Racoviteanu, A.E.; Walker, D.A. Landsat MSS-derived land-cover map of northern Alaska: Extrapolation methods and a comparison with photo-interpreted and AVHRR-derived maps. *Int. J. Remote Sens.* **1999**, *20*, 2921–2946. [CrossRef]
6. Tucker, C.J. Red and photographic infrared linear combinations for monitoring vegetation. *Remote Sens. Environ.* **1979**, *8*, 127–150. [CrossRef]
7. Epstein, H.E.; Raynolds, M.K.; Walker, D.A.; Bhatt, U.S.; Tucker, C.J.; Pinzon, J.E. Dynamics of aboveground phytomass of the circumpolar arctic tundra during the past three decades. *Environ. Res. Lett.* **2012**, *7*, 015506. [CrossRef]
8. Riedel, S.M.; Epstein, H.E.; Walker, D.A. Biotic controls over spectral reflectance of arctic tundra vegetation. *Int. J. Remote Sens.* **2005**, *26*, 2391–2405. [CrossRef]
9. Huemmrich, K.F.; Gamon, J.A.; Tweedie, C.E.; Oberbauer, S.F.; Kinoshita, G.; Houston, S.; Kuchy, A.; Hollister, R.D.; Kwon, H.; Mano, M. Remote sensing of tundra gross ecosystem productivity and light use efficiency under varying temperature and moisture conditions. *Remote Sens. Environ.* **2010**, *114*, 481–489. [CrossRef]

10. Hope, A.; Kimball, J.S.; Stow, D. The relationship between tussock tundra spectral reflectance properties and biomass and vegetation composition. *Int. J. Remote Sens.* **1993**, *14*, 1861–1874. [CrossRef]
11. Vierling, L.A.; Deering, D.W.; Eck, T.F. Differences in arctic tundra vegetation type and phenology as seen using bidirectional radiometry in the early growing season. *Remote Sens. Environ.* **1997**, *60*, 71–82. [CrossRef]
12. Laidler, G.J.; Treitz, P.; Atkinson, D. Remote sensing of arctic vegetation: Relations between the NDVI, spatial resolution and vegetation cover on Boothia Peninsula, Nunavut. *Arctic* **2008**, *61*, 1–13. [CrossRef]
13. Olthof, I.; Latifovic, R. Short-term response of arctic vegetation NDVI to temperature anomalies. *Int. J. Remote Sens.* **2007**, *28*, 4823–4840. [CrossRef]
14. Huemmrich, K.F.; Kinoshita, G.; Gamon, J.A.; Houston, S.; Kwon, H.; Oechel, W.C. Tundra carbon balance under varying temperature and moisture regimes. *J. Geophys. Res.* **2010**, *115*. [CrossRef]
15. Myers-Smith, I.H.; Forbes, B.C.; Wilmking, M.; Hallinger, M.; Lantz, T.; Blok, D.; Tape, K.D.; Macias-Fauria, M.; Sass-Klaassen, U.; Lévesque, E.; *et al*. Shrub expansion in tundra ecosystems: Dynamics, impacts and research priorities. *Environ. Res. Lett.* **2011**, *6*, 045509. [CrossRef]
16. Walker, D.A.; Epstein, H.E.; Jia, G.; Balser, A.; Copass, C.; Edwards, E.J.; Gould, W.A.; Hollingsworth, J.; Knudson, J.A.; Maier, H.A.; *et al*. Phytomass, LAI, and NDVI in northern Alaska: Relationships to summer warmth, soil pH, plant functional types, and extrapolation to the circumpolar Arctic. *J. Geophys. Res.* **2003**, *108*. [CrossRef]
17. Riedel, S.; Epstein, H.E.; Walker, D.A.; Richardson, D.L.; Calef, M.P.; Edwards, E.; Moody, A. Spatial and temporal heterogeneity of vegetation properties among four tundra plant communities at Ivotuk, Alaska, U.S.A. *Arct. Antarct. Alpine Res.* **2005**, *37*, 25–33. [CrossRef]
18. Buchhorn, M.; Walker, D.; Heim, B.; Raynolds, M.; Epstein, H.; Schwieder, M. Ground-based hyperspectral characterization of Alaska tundra vegetation along environmental gradients. *Remote Sens.* **2013**, *5*, 3971–4005. [CrossRef]
19. Ustin, S.L.; Gamon, J.A. Remote sensing of plant functional types. *New Phytol.* **2010**, *186*, 795–816. [CrossRef] [PubMed]
20. Curran, P.J. Remote sensing of foliar chemistry. *Remote Sens. Environ.* **1989**, *30*, 271–278. [CrossRef]
21. Vogelmann, J.E.; Moss, D.M. Spectral reflectance measurements in the genus *Sphagnum*. *Remote Sens. Environ.* **1993**, *45*, 273–279. [CrossRef]
22. Walker, D.A.; Epstein, H.E.; Raynolds, M.K.; Kuss, P.; Kopecky, M.A.; Frost, G.V.; Daniëls, F.J.A.; Leibman, M.O.; Moskalenko, N.G.; Matyshak, G.V.; *et al*. Environment, vegetation and greenness (NDVI) along the North America and Eurasia Arctic transects. *Environ. Res. Lett.* **2012**, *7*, 015504. [CrossRef]
23. Boelman, N.T.; Gough, L.; McLaren, J.R.; Greaves, H. Does NDVI reflect variation in the structural attributes associated with increasing shrub dominance in arctic tundra? *Environ. Res. Lett.* **2011**, *6*, 035501. [CrossRef]
24. Huemmrich, F.; Gamon, J.A.; Tweedie, C.E.; Campbell, P.; Landis, D.R.; Middleton, E. Arctic tundra vegetation functional types based on photosynthetic physiology and optical properties. *IEEE J. Sel. Top. Appl. Earth Obs. Remote Sens.* **2013**, *6*, 265–275. [CrossRef]
25. Xu, H.; Twine, T.; Yang, X. Evaluating remotely sensed phenological metrics in a dynamic ecosystem model. *Remote Sens.* **2014**, *6*, 4660–4686. [CrossRef]
26. DeMarco, J.; Mack, M.C.; Bret-Harte, M.S. Effects of arctic shrub expansion on biophysical *versus* biogeochemical drivers of litter decomposition. *Ecology* **2014**, *95*, 1861–1875. [CrossRef] [PubMed]
27. Winton, M. Amplified arctic climate change: What does surface albedo feedback have to do with it? *Geophys. Res. Lett.* **2006**, *33*. [CrossRef]
28. Serreze, M.C.; Francis, J.A. The arctic amplification debate. *Clim. Chang.* **2006**, *76*, 241–264. [CrossRef]
29. Kaufman, D.S.; Schneider, D.P.; McKay, N.P.; Ammann, C.M.; Bradley, R.S.; Briffa, K.R.; Miller, G.H.; Otto-Bliesner, B.L.; Overpeck, J.T.; Vinther, B.M.; *et al*. Recent warming reverses long-term arctic cooling. *Science* **2009**, *325*, 1236–1239. [CrossRef] [PubMed]
30. Comiso, J.C.; Hall, D.K. Climate trends in the Arctic as observed from space. *Wiley Interdiscip. Rev.* **2014**, *5*, 389–409. [CrossRef] [PubMed]
31. Hansen, J.; Ruedy, R.; Sato, M.; Lo, K. Global surface temperature change. *Rev. Geophys.* **2010**, *48*. [CrossRef]
32. Bhatt, U.S.; Walker, D.A.; Raynolds, M.K.; Comiso, J.C.; Epstein, H.E.; Jia, G.; Gens, R.; Pinzon, J.E.; Tucker, C.J.; Tweedie, C.E.; *et al*. Circumpolar arctic tundra vegetation change is linked to sea ice decline. *Earth Interact.* **2010**, *14*, 1–20. [CrossRef]

33. Zeng, H.; Jia, G.; Epstein, H. Recent changes in phenology over the northern high latitudes detected from multi-satellite data. *Environ. Res. Lett.* **2011**, *6*, 045508. [CrossRef]
34. Jia, G.J.; Epstein, H.E.; Walker, D.A. Controls over intra-seasonal dynamics of AVHRR NDVI for the arctic tundra in northern Alaska. *Int. J. Remote Sens.* **2004**, *25*, 1547–1564. [CrossRef]
35. Hinzman, L.D.; Deal, C.J.; McGuire, A.D.; Mernild, S.H.; Polyakov, I.V.; Walsh, J.E. Trajectory of the arctic as an integrated system. *Ecol. Appl.* **2013**, *23*, 1837–1868. [CrossRef] [PubMed]
36. Elmendorf, S.C.; Henry, G.H.; Hollister, R.D.; Bjork, R.G.; Bjorkman, A.D.; Callaghan, T.V.; Collier, L.S.; Cooper, E.J.; Cornelissen, J.H.; Day, T.A.; *et al*. Global assessment of experimental climate warming on tundra vegetation: Heterogeneity over space and time. *Ecol. Lett.* **2012**, *15*, 164–175. [CrossRef] [PubMed]
37. Sturm, M.; Racine, C.; Tape, K.D. Increasing shrub abundance in the Arctic. *Nature* **2001**, *411*, 1251–1256. [CrossRef] [PubMed]
38. Tape, K.E.N.; Sturm, M.; Racine, C. The evidence for shrub expansion in northern Alaska and the pan-Arctic. *Glob. Chang. Biol.* **2006**, *12*, 686–702. [CrossRef]
39. Sturm, M.; McFadden, J.P.; Liston, G.E.; Chapin, F.S., III; Racine, C.; Holmgren, J. Snow-shrub interactions in arctic tundra: A hypothesis with climate implications. *J. Clim.* **2001**, *14*, 336–344. [CrossRef]
40. Raynolds, M.K.; Walker, D.A.; Epstein, H.E.; Pinzon, J.E.; Tucker, C.J. A new estimate of tundra-biome phytomass from trans-arctic field data and AVHRR NDVI. *Remote Sens. Lett.* **2012**, *3*, 403–411. [CrossRef]
41. Forbes, B.C.; Fauria, M.M.; Zetterberg, P. Russian arctic warming and "greening" are closely tracked by tundra shrub willows. *Glob. Chang. Biol.* **2010**, *16*, 1542–1554. [CrossRef]
42. Jia, G.J.; Epstein, H.E.; Walker, D. Spatial characteristics of AVHRR-NDVI along latitudinal transectsin northern alaska. *J. Veg. Sci.* **2002**, *13*, 315–326. [CrossRef]
43. CAVM. *Circumpolar Arctic Vegetation Map. (1:7,500,000 Scale), Conservation of Arctic Flora and Fauna (Caff) Map No. 1*; U.S. Fish and Wildlife Service: Anchorage, AK, USA, 2003.
44. Walker, D.; Raynolds, M.; Daniels, F.J.A.; Einarsson, E.; Elvebakk, A.; Gould, W.A.; Katenin, A.E.; Kholod, S.S.; Markon, C.J.; Yurstev, B.A. The Circumpolar Arctic Vegetation Map. *J. Veg. Sci.* **2005**, *16*, 267–282. [CrossRef]
45. Murray, D.F. Vegetation, floristics, and phytogeography of northern Alaska. In *Vegetation and Production Ecology of an Alaskan Arctic Tundra*; Tieszen, L.L., Ed.; Springer-Verlag: New York, NY, USA, 1978; pp. 19–36.
46. Walker, M.D.; Walker, D.; Auerbach, N.A. Plant communities of a tussock tundra landscape in the Brooks Range foothills, Alaska. *J. Veg. Sci.* **1994**, *5*, 843–866. [CrossRef]
47. Shaver, G.R.; Chapin, F.S. Production: Relationships and element cycling in contrasting arctic vegetation types. *Ecol. Monogr.* **1991**, *61*, 1–31. [CrossRef]
48. Walker, D.; Bockheim, J.G.; Chapin, F.S.; Eugster, W.; Nelson, F.; Ping, C.L. Calcium-rich tundra, wildlife, and the "mammoth steppe". *Quat. Sci. Rev.* **2001**, *20*, 149–163. [CrossRef]
49. Walker, D.; Auerbach, N.A.; Bockheim, J.G.; Chapin, F.S.; Eugster, W.; King, J.Y.; McFadden, J.P.; Michaelson, G.J.; Nelson, F.; Oechel, W.C.; *et al*. Energy and trace-gas fluxes across a soil pH boundary in the Arctic. *Nature* **1998**, *394*, 469–472. [CrossRef]
50. Walker, D.; Auerbach, N.A.; Shippert, M. NDVI, biomass, and landscape evolution of glaciated terrain in northern Alaska. *Polar Rec.* **1995**, *31*, 169–178. [CrossRef]
51. Raynolds, M.; Walker, D. Effects of deglaciation on circumpolar distribution of arctic vegetation. *Can. J. Remote Sens.* **2009**, *35*, 118–129. [CrossRef]
52. Bliss, L.C.; Matveyeva, N.V. Circumpolar arctic vegetation. In *Arctic Ecosystems in a Changing Climate*; Chapin, F.S., III, Jefferies, R.L., Reynolds, A., Shaver, G.R., Svoboda, J., Eds.; Academic Press, Inc.: San Diego, CA, USA, 1992.
53. Tenhunen, J.D.; Lange, O.L.; Hahn, S.; Siegwolf, R.; Oberbauer, S.F. The ecosystem role of poikilohydric tundra plants. In *Arctic Ecosystems in a Changing Climate: An Ecosphysiological Perspective*; Chapin, F.S., III, Jefferies, R.L., Reynolds, J.F., Shaver, G.R., Eds.; Academic Press, Inc.: San Diego, CA, USA, 1992; pp. 213–239.
54. Epstein, H.E.; Calef, M.P.; Walker, M.D.; Chapin, F.S., III; Starfield, A.M. Detecting changes in arctic tundra plant communities in response to warming over decadal time scales. *Glob. Chang. Biol.* **2004**, *10*, 1325–1334. [CrossRef]
55. McGuire, A.D. Arctic transitions in the land-atmosphere system (atlas): Background, objectives, results, and future directions. *J. Geophys. Res.* **2003**, *108*. [CrossRef]

56. Walker, D.A.; Jia, G.J.; Epstein, H.E.; Raynolds, M.K.; Chapin, F.S., III; Copass, C.; Hinzman, L.D.; Knudson, J.A.; Maier, H.A.; Michaelson, G.J.; *et al*. Vegetation-soil-thaw-depth relationships along a low-arctic bioclimate gradient, Alaska: Synthesis of information from the ATLAS studies. *Permafr. Periglac. Process.* **2003**, *14*, 103–123. [CrossRef]
57. Epstein, H.E.; Walker, D.A.; Raynolds, M.K.; Jia, G.J.; Kelley, A.M. Phytomass patterns across a temperature gradient of the North American arctic tundra. *J. Geophys. Res.* **2008**, *113*. [CrossRef]
58. Chapin, F.S.; Shaver, G.R.; Giblin, A.E.; Nadelhoffer, K.J.; Laundre, J.A. Responses of arctic tundra to experimental and observed changes in climate. *Ecology* **1995**, *76*, 694–711.
59. Hobbie, S.E.; Shevtsova, A.; Chapin, F.S., III. Plant responses to species removal and experimental warming in Alaskan tussock tundra. *Oikos* **1999**, *84*, 417–434. [CrossRef]
60. Atlas Project Website. Available online: http://www.eol.ucar.edu/projects/atlas/ivotuk_cd/html/IvotukFrameset.htm (accessed on 1 September 2015).
61. Kade, A.; Walker, D.A.; Raynolds, M.K. Plant communities and soils in cryoturbated tundra along a bioclimate gradient in the low arctic, Alaska. *Phytocoenologia* **2005**, *35*, 761–820. [CrossRef]
62. Raynolds, M.K.; Walker, D.A.; Munger, C.A.; Vonlanthen, C.M.; Kade, A.N. A map analysis of patterned-ground along a North American arctic transect. *J. Geophys. Res.* **2008**, *113*. [CrossRef]
63. Walker, D.; Kuss, P.; Epstein, H.E.; Kade, A.N.; Vonlanthen, C.M.; Raynolds, M.; Daniëls, F.J.A. Vegetation of zonal patterned-ground ecosystems along the North America Arctic bioclimate gradient. *Appl. Veg. Sci.* **2011**, *14*, 440–463. [CrossRef]
64. Walker, D.; Epstein, H.E.; Romanovsky, V.E.; Ping, C.L.; Michaelson, G.J.; Daanen, R.P.; Shur, Y.L.; Peterson, R.A.; Krantz, W.B.; Raynolds, M.; *et al*. Arctic patterned-ground ecosystems: A synthesis of field studies and models along a North American Arctic Transect. *J. Geophys. Res.* **2008**, *113*, 1–17. [CrossRef]
65. Strauss, J.; Buchhorn, M. *Expeditions to the Permafrost 2012: Alaskan North Slope/Itkilik, thermokarst in Central Yakutia, EyeSight-NAAT-Alaska*; Alfred-Wegener-Institut für Polar-und Meeresforschung: Bremerhaven, Germany, 2012.
66. Clark, R.N.; Roush, T.L. Reflectance spectroscopy: Quantitative analysis techniques for remote sensing applications. *J. Geophys. Res.* **1984**, *89*, 6329–6340. [CrossRef]
67. Kokaly, R.F.; Skidmore, A.K. Plant phenolics and absorption features in vegetation reflectance spectra near 1.66 μm. *Int. J. Appl. Earth Obs. Geoinform.* **2015**. [CrossRef]
68. Marshall, G.J.; Thenkabail, P. Biomass modeling of four leading world crops using hyperspectral narrowbands in support of HyspIRI mission. *Photogramm. Eng. Remote Sens.* **2014**, *80*, 757–772. [CrossRef]
69. Hughes, M. On the mean accuracy of statistical pattern recognizers. *IEEE Trans. Inf. Theory* **1968**, *14*, 55–63. [CrossRef]
70. Chung, D.; Chun, H.; Keles, S. *Spls: Sparse Partial Least Squares (spls) Regression and Classification*; R Package Vignette: Madison, WI, USA, 2013.
71. Chun, H.; Keles, S. Sparse partial least squares regression for simultaneous dimension reduction and variable selection. *J. Royal Stat. Soc. Ser. B (Methodol.)* **2010**, *72*, 3–25. [CrossRef] [PubMed]